IEEE Photonics Journal
An IEEE Photonics Society Publication

Open Access

Surface Antireflection and Light Extraction Properties of GaN Microdomes

Volume 7, Number 2, April 2015

Lu Han
Roger H. French
Hongping Zhao

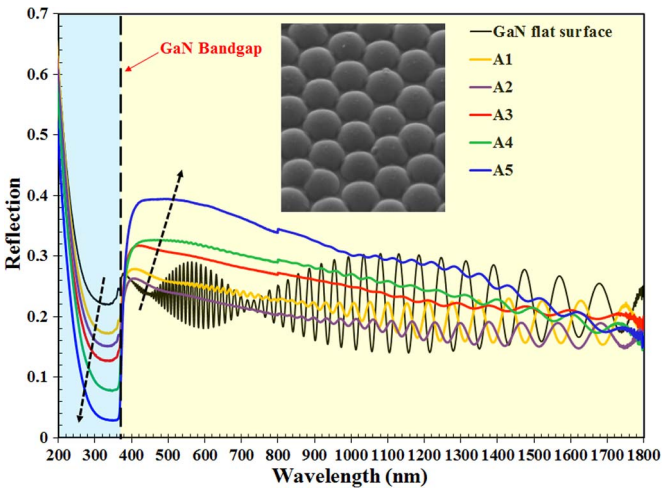

DOI: 10.1109/JPHOT.2015.2403353
1943-0655 © 2015 IEEE

IEEE photonics SOCIETY

IEEE

Surface Antireflection and Light Extraction Properties of GaN Microdomes

Lu Han,[1] Roger H. French,[2] and Hongping Zhao[1]

[1]Department of Electrical Engineering and Computer Science, Case Western Reserve University, Cleveland, OH 44106 USA
[2]Department of Materials Science and Engineering, Case Western Reserve University, Cleveland, OH 44106-7204 USA

DOI: 10.1109/JPHOT.2015.2403353
1943-0655 © 2015 IEEE. Translations and content mining are permitted for academic research only. Personal use is also permitted, but republication/redistribution requires IEEE permission. See http://www.ieee.org/publications_standards/publications/rights/index.html for more information.

Manuscript received January 6, 2015; revised February 6, 2015; accepted February 9, 2015. Date of publication February 13, 2015; date of current version February 19, 2015. This work was supported through start-up funds from Case Western Reserve University. Corresponding author: H. Zhao (e-mail: hongping.zhao@case.edu).

Abstract: GaN microdomes were fabricated and measured as both an antireflection surface and a light extraction enhancement structure. The combination of self-assembled micro/nanosphere lithography and reactive ion etching process was used to fabricate GaN microdomes with different aspect ratios. SiO_2 microspheres with diameters of 1000 and 500 nm, deposited on top of the GaN substrate using a dip-coating method, serve as the mask for the formation of GaN microdomes. The GaN microdome shapes and sizes were determined through control of the plasma etching conditions. The antireflection properties of the GaN microdomes with different sizes and shapes were characterized. Two different mechanisms were proposed to explain the surface reflection properties of incidence wavelength below and above GaN band gap, respectively. The trend shows that the surface reflection is reduced with the increase in the aspect ratio of the GaN microdomes for incidence wavelength above the band gap. For incidence wavelength below the band gap, the trend is totally different. Studies indicate that the microdomes are applicable not only as antireflection structures in solar cells but for enhancing light extraction in light-emitting diodes as well.

Index Terms: Light-emitting diodes (LEDs), light-matter interactions, photovoltaics, photonic materials.

1. Introduction

III-nitride semiconductors (Al, In, Ga, -N) have been commercially applied in light-emitting diodes (LEDs) [1]–[3], laser diodes [4], [5], and potentially concentrator photovoltaics (CPVs) [6]–[8]. The wide band gap tuning of III-nitrides ranging from deep-ultraviolet (UV) up to near infrared provides great promise for high efficiency solar cell device application. One common issue associated with the inorganic semiconductor based optoelectronic devices is the photon energy loss at the interface between the semiconductor and the ambient medium, due to the large contrast of the refractive index [9]. Antireflection coatings with appropriate refractive index have been used in solar cell devices to reduce the surface reflection [10]. However, traditional antireflection coatings provide minimum surface reflection only at a single wavelength with normal incidence angle light. Surface texturing is an effective approach to reduce interface photon energy loss in both LEDs and solar cell devices [11]–[15].

Recently, GaN microdomes have been studied as an effective surface structure that leads to significant enhancement of light extraction efficiency in both InGaN quantum wells (QWs) based visible LEDs [14] and AlGaN QWs based UV/deep-UV LEDs [15]. In contrast to the traditional technology based on surface roughness for LED light extraction efficiency enhancement, the use of microdome surface structure allows the formation of uniform and controllable shape surface structures. Our recent numerical simulation studies indicate the GaN microdomes can also serve as effective antireflection surface structures [16]. The results indicate that surface reflection has a significant dependence on the surface geometrical structure and that it can provide broadband omnidirectional antireflection for both P and S polarizations. Very recently, we have demonstrated the feasibility of fabricating GaN microdomes based on the self-assembled micro/nanosphere lithography and plasma etching approach [17].

In this work, we comprehensively studied the dependence of the plasma etching process on the GaN microdome surface geometrical shape and the corresponding surface reflection properties. Specifically, two mechanisms were proposed to explain the surface reflection properties of the incidence wavelength of above and below GaN band gap. With the incidence wavelength above the band gap, the trend indicates the reduction of surface reflection as the increase of the aspect ratio of the GaN microdomes. With incidence wavelength below the GaN band gap, the trend is very different.

2. Fabrication of GaN Microdomes with Different Aspect Ratios

In this study, GaN microdomes were fabricated by using a reactive ion etching (RIE) process, during which the self-assembled SiO_2 microspheres serve as the mask [18], [19]. The simultaneous etching of SiO_2 mask and GaN leads to the formation of GaN microdomes. SiO_2 microspheres were deposited as hexagonal close-packed monolayer on GaN substrate utilizing the self-assembled dip-coating method. The detailed process was described in our previous work [17]. Here, we mainly focus on the study of the effect of plasma etching process on the GaN microdome size, shape and aspect ratio. Note that the RIE process is a standard process for the fabrication of III-nitride based LEDs or solar cell devices.

By controlling the RIE etching conditions, the structural parameters of GaN microdomes including the shape, size and aspect ratio can be well controlled. Using appropriate etching gases (e.g., chlorine based and fluorine based), the etching rates of GaN and SiO_2 microspheres can be well tuned, which in turn determines the shape of the GaN microdomes. Here, Cl_2 and SF_6 were selected as etching gases to selectively etch GaN and SiO_2 microspheres, respectively [20]–[22]. By controlling the ratio of these two etching gases, GaN microdomes with different aspect ratios were obtained. The etching process was performed utilizing a Lam Research 9400 Etcher with RF power of 500 W and bias voltage of 108 V. The chamber pressure was set as 10 mTorr.

Note that the technology of surface patterning for either LED or solar cell device applications requires the consideration of the feasibility and potential effect from processing on device performance. For devices with relatively thin ($\sim$300–500 nm) top layer thickness, small surface feature size is preferred. For devices with relatively thick (3–5 μm) top layer thickness such as flip-chip LEDs, the surface feature size has a broader range of selection. Here, we study two cases: 1) microdome diameter of 1000 nm; and 2) microdome diameter of 500 nm. The study of the surface antireflection properties of GaN microdomes can be applied to different material system and devices including Si-based, III-V based or organic based optoelectronic devices.

Table 1 lists the five different RIE conditions for the GaN substrates with deposited a monolayer of SiO_2 microspheres with diameters of 1000 nm. By fixing the Cl_2 flow rate of 48 sccm and adjusting the SF_6 flow rate from 37 down to 10 sccm, we observe the etching rate ratio of GaN/SiO_2 increases. The lower flow rate of SF_6 will lead to the increase of the aspect ratio of the GaN microdomes. Table 1 also lists the corresponding estimated GaN microdome height for each case. From the experiment, the gas flow rate ratio of Cl_2/SF_6 significantly affects the GaN/SiO_2 etching rate ratio, which in turn determines the aspect ratio of the GaN microdome structures.

TABLE 1

RIE conditions for five samples (A1, A2, A3, A4, and A5) of GaN substrates deposited with SiO_2 microspheres with diameter of 1000 nm

Sample ID	Gas Flow Rates (sccm)		Etching Time	Microdome Height (nm)
	Cl_2	SF_6		
A1	48	37	8'	420
A2	48	32	8'	580
A3	48	24	9'10"	1180
A4	48	20	9'20"	1380
A5	48	10	9'45"	2050

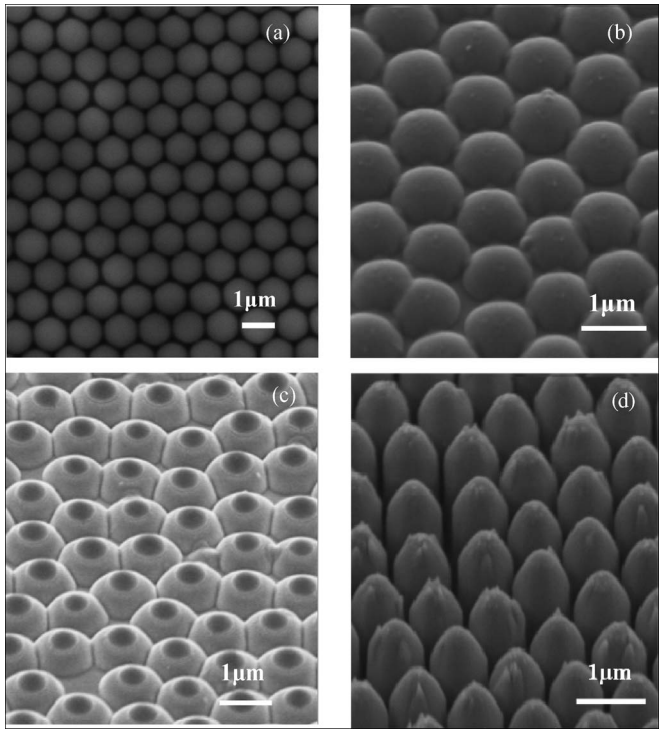

Fig. 1. (a) SEM image of the hexagonal close-packed SiO_2 microspheres with diameter of 1000 nm as a close-packed monolayer deposited on the GaN substrate prior to the RIE process. (b)–(d) 45° tilted SEM images of GaN microdome structures for sample A1, A2, and A5, respectively, formed via three different RIE etching conditions listed in Table 1.

Fig. 1(a) shows a scanning electron microscopy (SEM) image of the hexagonal close-packed SiO_2 microspheres with 1000 nm diameter deposited on the GaN substrate via dip coating method [17]. Fig. 2(b)–(d) show the 45° tilted SEM images of the GaN microdome structures for sample A1, A2, and A5, respectively, formed via three different RIE etching conditions, as listed in Table 1.

Note that during the plasma etching process, the Cl_2 gas mainly reacts with GaN located at the void area between the SiO_2 microspheres. Meanwhile, SF_6 reacts with SiO_2 which leads to the shrinkage of the SiO_2 sphere size. Thus, with the mixture of the Cl_2 and SF_6 gases, the GaN microdomes are formed. The shape and size can be tuned based on the etching rates of GaN and SiO_2. From Fig. 1, GaN microdomes with different aspect ratios were formed with different flow rates of SF_6 and fixed Cl_2 flow rate. With higher flow rate of SF_6, the SiO_2 etching rate is faster which leads to GaN microdomes with smaller height as shown in Fig. 1(b). In Fig. 1(c), on top of

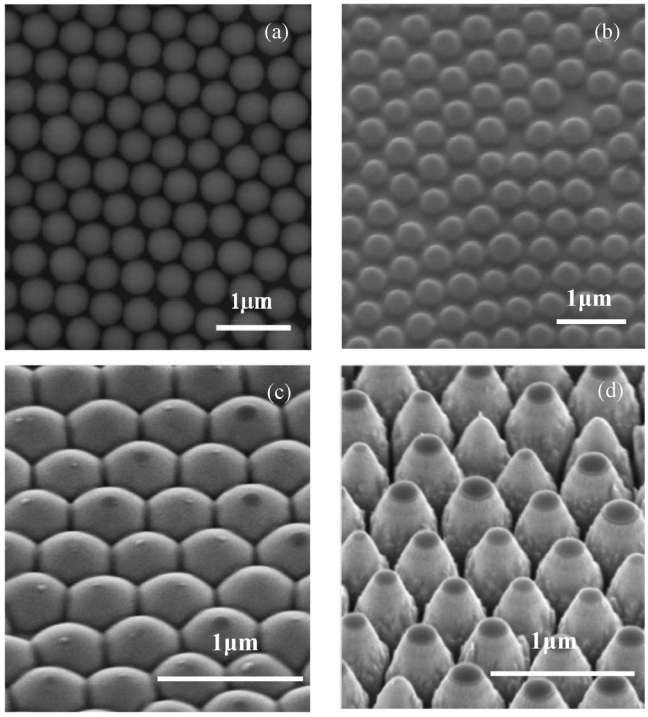

Fig. 2. (a) SEM image of the hexagonal close-packed SiO_2 microspheres with diameter of 500 nm deposited on GaN substrate prior RIE process. (b)–(d) 45° tilted SEM images of GaN microdome structures for sample B1, B2, and B5, respectively, formed via three different RIE etching conditions listed in Table 2.

TABLE 2

RIE conditions for five samples (B1, B2, B3, B4, and B5) of GaN substrates deposited with SiO_2 microspheres with diameter of 500 nm

Sample ID	Gas Flow Rates (sccm)		Etching Time	Microdome Height (nm)
	Cl_2	SF_6		
B1	48	35	6'	80
B2	48	32	4'10″	250
B3	48	20	4'30"	490
B4	48	18	4'35"	800
B5	48	15	4'30"	990

the GaN microdomes, there remains of SiO_2 microspheres, which could be etched away with longer etching time.

Table 2 lists the five different RIE conditions for GaN substrates deposited with close-packed SiO_2 microspheres with diameter of 500 nm. The dip coating condition for SiO_2 microspheres with smaller diameter of 500 nm differs from that of 1000 nm [17]. Similar to the case of SiO_2 microsphere with 1000 nm, the RIE etching conditions vary by tuning SF_6 flow rates from 35 sccm down to 15 sccm with fixed Cl_2 flow rate of 48 sccm. The corresponding estimated GaN microdome heights for each case are also listed in Table 2. Similar trend was observed here as the case listed in Table 1: as the increase of the flow rate ratio of Cl_2/SF_6, the aspect ratio of the GaN microdomes increases.

Fig. 2(a) shows SEM image of the hexagonal close-packed SiO_2 microspheres with diameter of 500 nm deposited on a GaN substrate via dip-coating method. Fig. 2(b)–(d) show the 45° tilted SEM images of the GaN microdome structures for sample B1, B2, and B5, respectively,

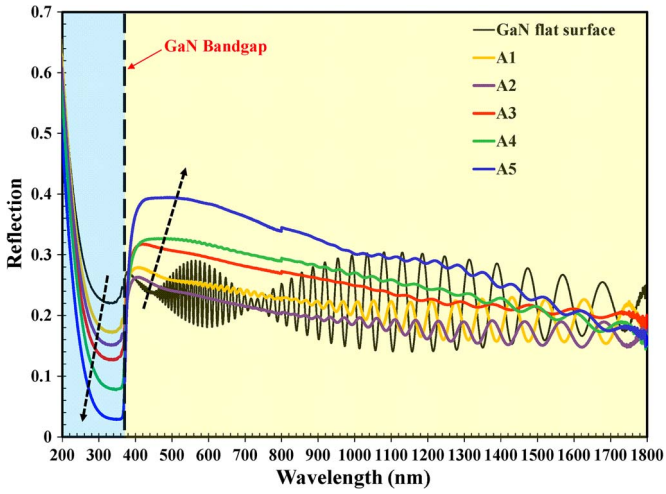

Fig. 3. Total surface reflection of GaN microdomes with diameter of 1000 nm for the samples of A1, A2, A3, A4, and A5, as compared to the GaN flat surface.

formed via three different RIE etching conditions listed in Table 2. As compared to the case of SiO_2 with 1000 nm diameter, the etching time here is shorter. With a Cl_2 flow rate of 48 sccm and SF_6 flow rate of 35 sccm, the formed GaN microdomes contain structure height of 80 nm as shown in Fig. 2(b), which is due to the relatively fast etching rate of SiO_2. With a Cl_2 flow rate of 48 sccm and SF_6 flow rate of 15 sccm, the formed GaN microdomes as shown in Fig. 2(d) have relative large aspect ratio with height of 990 nm. Note that there exists SiO_2 residue on top of the GaN microdomes, which could be removed with longer etching time.

3. Surface Reflection Characterizations of GaN Microdomes

The surface reflection properties of GaN microdomes with various sizes and aspect ratios were characterized using a Cary 6000i UV-VIS-NIR Spectrophotometer. The Cary 6000i was used to collect the total reflectance from the sample, which includes both specular reflectance and diffuse reflectance. The total reflection was collected by an integrating sphere. The surface reflection measurements were taken with the broad wavelength range from 188 to 1800 nm with a fixed incidence angle of 4°. Based on our previous studies, the total surface reflection increases as incidence angle increases [16]. In this study, the measurements based on 4° of incidence angle are representative and the results are similar to the case for normal incidence angle.

From our previous simulation studies, the size and shape of surface structures significantly affect the surface reflection properties [16]. Here, GaN microdomes formed with SiO_2 microspheres with diameters of both 1000 nm and 500 nm were characterized as compared to that of the conventional GaN flat surface. Fig. 3 shows the total surface reflection as a function of the incidence wavelength for the six GaN microdome samples (A1–A5) compared to that of the GaN flat surface. Note that all of the GaN samples were grown on top of the sapphire substrate. The thickness of the GaN layer is about 5 μm. From Fig. 3, we observe two different trends separated by the band gap of GaN (3.42 eV, or 362 nm). With the incidence wavelength above the band gap, the surface reflection reduces as the increase of the aspect ratio of the GaN microdomes. For the incidence wavelength below the band gap, the surface reflection shows a totally different trend.

In Fig. 3, for the conventional GaN flat surface, the surface reflection shows a strong interference fringe as a function of the incident wavelength. While for the GaN microdome samples, the interference fringe does not show a continuous oscillation as a function of the wavelength. With the two interfaces between air/GaN and GaN/sapphire, the reflected waves from upper interface and lower interface interferes. For the GaN flat surface with parallel interfaces, the phase

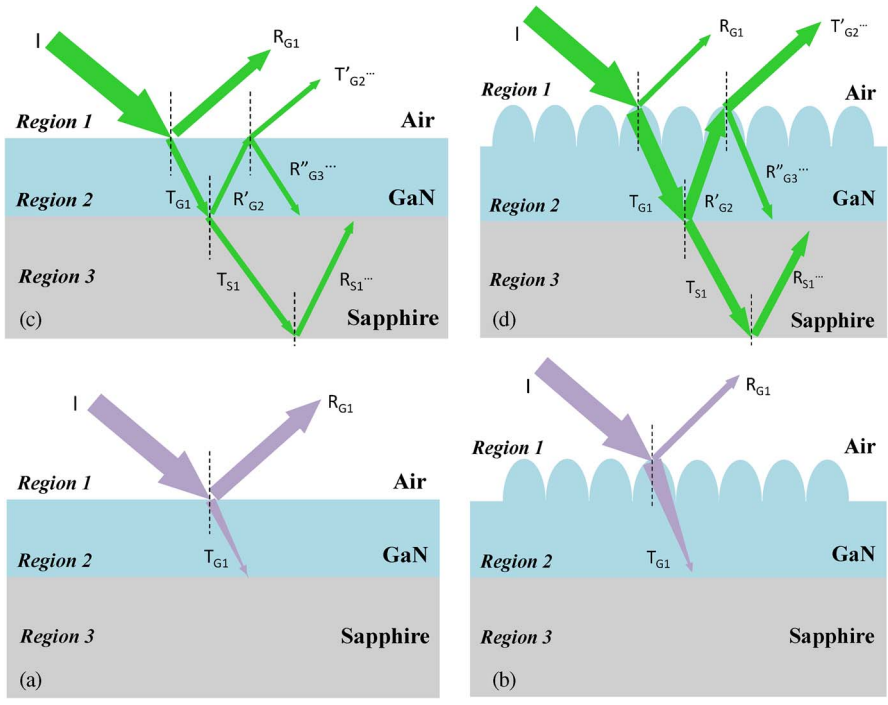

Fig. 4. Schematics of the total surface reflection for GaN flat surface with incidence wavelength (a) above and (c) below the GaN band gap and for GaN microdome structures (b) above and (d) below the GaN band gap.

difference between the two reflected waves continuously change as a function of the incidence wavelength. While for the microdome structure, the phase difference between the reflected waves does not change continuously as a function of the incidence wavelength.

In order to explain the mechanism of the surface reflection properties shown in Fig. 3, we plot the two different scenarios in Fig. 4, in which Fig. 4(a) and (b) represent the case for incidence wavelength above the GaN band gap. Fig. 4(c) and (d) represent the case for incidence wavelength below the GaN band gap. With the incidence wavelength in the UV region [Fig. 4(a) and (b)], the incident photons (I) are partially reflected at the interface (R_{G1}) and partially transmitted into the GaN layer (T_{G1}). Since the GaN layer thickness is $\sim 5\mu$m, the majority of the transmitted photons are absorbed by GaN layer. Thus, the total surface reflection is dominated by the initial surface reflection R_{G1}. The GaN microdome structures lead to enhancement of the coupling efficiency of the incident photon energy, which results in the reduction of the surface reflection as shown in Fig. 3. With the increase of the aspect ratio of the GaN microdomes, the total surface reflection reduces $(\lambda < 362$ nm$)$. Sample A5 shows the lowest surface reflection ($\sim$2%) with the incidence wavelength of 320–360 nm.

With the incidence wavelength longer than the GaN band gap [Fig. 4(c) and (d)], the incident photons are partially reflected at the interface (R_{G1}) and partially transmitted into the GaN layer (T_{G1}). Since the incident wavelength is below the GaN band gap, which will not be absorbed by the GaN layer. The transmitted photons will be partially reflected at the GaN/sapphire interface $(R_{\prime G2})$, which again will be partially reflected $(R_{\prime G3})$ and transmitted $(T_{\prime G2})$ at the GaN/medium interface. Thus, with the incidence wavelength below the GaN band gap, the total surface reflection is composed of both initial surface reflection $(R_{\prime G1})$ and multiple secondary transmissions $(T_{\prime G2})$ from GaN to the medium, which represents a more complex process. Note that the GaN microdomes not only lead to the reduction of surface reflection but lead to enhancement of the light extraction efficiency as well. The total surface reflection will then be determined by the multiple components of the reflection (R_{G1}) and transmission $(T_{\prime G2...})$ at the GaN/medium interface.

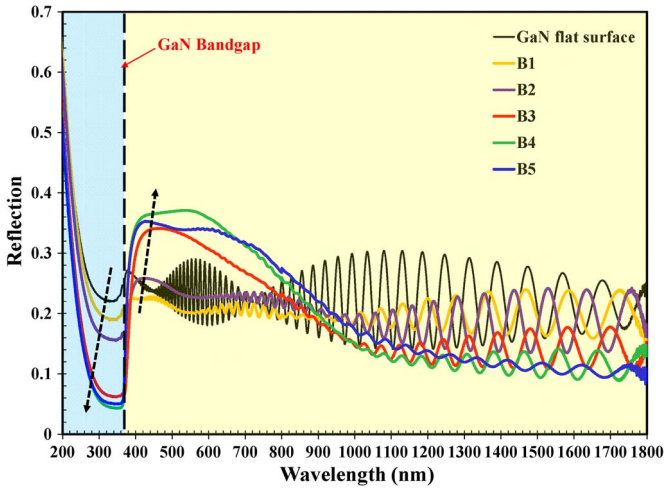

Fig. 5. Total surface reflection of GaN microdomes with diameter of 1000 nm for the samples of B1, B2, B3, B4, and B5, as compared to the GaN flat surface.

In Fig. 3, sample A5 shows the highest surface reflection below the GaN band gap, which is opposite of the trend for above the band gap. This indicates that the light extraction components $(T'G2\ldots)$ dominate the total surface reflection, instead of the initial surface reflection (R_{G1}). From this, we can conclude that GaN microdomes are also effective surface texturing for enhancing LED light extraction efficiency.

Similarly, Fig. 5 plots the total surface reflection as a function of incidence wavelength for the GaN microdomes with diameter of 500 nm. Fig. 5 shows the similar trend as that of Fig. 3: with the incidence wavelength above the GaN band gap, the surface reflection reduces as the increase of the aspect ratio of the GaN microdomes; for incidence wavelength below the GaN band gap, the surface reflection shows the general trend of the increase of surface reflection. Note that the total surface reflection for incidence wavelength below the band gap is the combination of initial surface reflection and multiple light extraction components.

By comparing the two cases we studied above with microspheres D = 1000 nm and D = 500 nm, we observe a similar trend: As the aspect ratio of the microdomes increases, the surface reflection reduces. The studies indicate the fabrication approach based on the simultaneous etching of SiO_2 microspheres and GaN to control the GaN microdome shape is feasible for both micro- and submicro-feature size. Indeed, this approach should be applicable for applications that require even smaller feature size.

To better compare the dependence of surface reflection on the GaN microdome aspect ratio. Fig. 6 plots the measured surface reflection at incidence wavelength of 350 nm as a function of the GaN microdome aspect ratio. H/D = 0 represents the case for a GaN flat surface. With incident wavelength of 350 nm, the conventional GaN flat surface shows reflection of 22%. From Fig. 6, the surface reflection reduces as the increase of the GaN microdomes for both GaN microdome diameters of 1000 nm and 500 nm. This measurement results matches with our previous simulation studies [16].

For solar cell or photodetector device applications, only incident photons of wavelengths that are shorter than the semiconductor band gap will contribute to the conversion of photon energy to electrical energy. On one hand, the pattern of the surface with microdome structures will lead to the enhancement of the absorption of photons with wavelength above the band gap, which will result in the enhancement of device efficiency. On the other hand, the GaN microdomes could reduce the trapping of the unabsorbed photons with wavelength below the band gap. This could potentially reduce the temperature of the solar cell or photodetector devices. From this study, the microdome structures can also be implemented in LED devices to enhance light extraction efficiency.

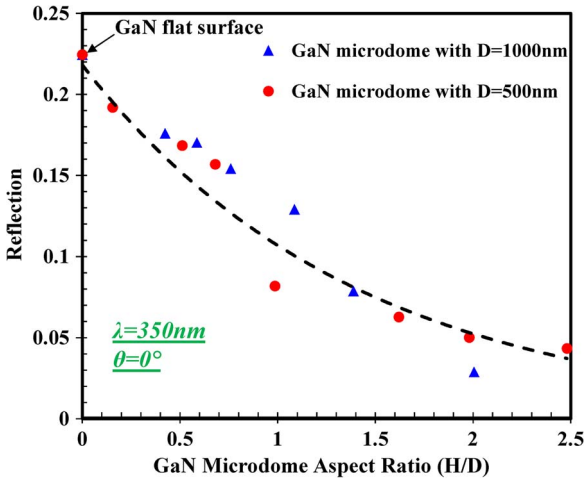

Fig. 6. Measurement comparison of surface reflection of GaN microdomes with diameter 1000 nm (blue triangle) and 500 nm (red circle) as a function of structure aspect ratio, height over diameter (H/D), at wavelength of 350 nm.

4. Summary

In summary, we have demonstrated the fabrication of GaN microdome structures via the RIE process using SiO_2 microspheres as mask. The tuning of the GaN microdomes aspect ratio can be achieved by control the plasma etching condition. The surface reflection properties show significant dependence on the GaN microdome aspect ratio. Experimental results reveal that GaN microdomes not only serve as an effective surface structure for enhancing light collection efficiency in solar cell devices, but also could lead to significant enhancement for light extraction efficiency in LED devices. With the low cost and controllable approach for fabrication of GaN microdomes, this surface texturing technology could be implemented in optoelectronic devices to enhance device efficiency.

References

[1] J. Liu *et al.*, "Green light-emitting diodes with pInGaN: Mg grown on C-plane sapphire and GaN substrates," *Phys. Status Solidi, A Appl. Mater. Sci.*, vol. 206, no. 4, pp. 750–753, 2009.
[2] N. G. Toledo and U. K. Mishra, "InGaN solar cell requirements for high-efficiency integrated III-nitride/non-III-nitride tandem photovoltaic devices," *J. Appl. Phys.*, vol. 111, no. 11, Jun. 2012, Art. ID. 114505.
[3] J. Han and A. V. Nurmikko, "Advances in AlGaInN blue and ultraviolet light emitters," *IEEE J. Sel. Topics Quantum Electron.*, vol. 8, no. 2, pp. 289–297, Mar./Apr. 2002.
[4] D. Queren *et al.*, "500 nm electrically driven InGaN based laser diodes," *Appl. Phys. Lett.*, vol. 94, no. 8, Feb. 2009, Art. ID. 081119.
[5] M. Kneissl, D. W. Treat, M. Teepe, N. Miyashita, and N. M. Johnson, "Continuous-wave operation of ultraviolet InGaN/InAlGaN multiple-quantum-well laser diodes," *Appl. Phys. Lett.*, vol. 82, no. 15, pp. 2386–2388, Apr. 2003.
[6] C. J. Neufeld *et al.*, "High quantum efficiency InGaN/GaN solar cells with 2.95 eV band gap," *Appl. Phys. Lett.*, vol. 93, no. 14, Oct. 2008, Art. ID. 143502.
[7] R. Dahal, B. Pantha, J. Li, J. Y. Lin, and H. X. Jiang, "InGaN/GaN multiple quantum well solar cells with long operating wavelengths," *Appl. Phys. Lett.*, vol. 94, no. 6, Feb. 2009, Art. ID. 063505.
[8] O. Jani, I. Ferguson, C. Honsberg, and S. Kurtz, "Design and characterization of GaN/InGaN solar cells," *Appl. Phys. Lett.*, vol. 91, no. 13, Sep. 2007, Art. ID. 132117.
[9] P. Zhu, G. Liu, J. Zhang, and N. Tansu, "FDTD analysis on extraction efficiency of GaN light-emitting diodes with microsphere arrays," *J. Display Technol.*, vol. 9, no. 5, pp. 317–323, May 2013.
[10] J.-Q. Xi *et al.*, "Optical thin-film materials with low refractive index for broadband elimination of Fresnel reflection," *Nature Photon.*, vol. 1, pp. 176–179, Mar. 2007.
[11] C. H. Chiu *et al.*, "Broadband and omnidirectional antireflection employing disordered GaN nanopillars," *Opt. Exp.*, vol. 16, no. 12, pp. 8748, Jun. 2008.
[12] R. Dewan *et al.*, "Studying nanostructured nipple arrays of moth eye facets helps to design better thin film solar cells," *Bioinspiration Biomim.*, vol. 7, no. 1, Mar. 2012, Art. ID. 016003.
[13] Y. K. Ee, R. A. Arif, N. Tansu, P. Kumnorkaew, and J. F. Gilchrist, "Enhancement of light extraction efficiency of InGaN quantum wells light emitting diodes using SiO_2/polystyrene microlens arrays," *Appl. Phys. Lett.*, vol. 91, no. 22, Nov. 2007, Art. ID. 221107.

[14] P. Zhao and H. Zhao, "Analysis of light extraction efficiency enhancement for thin-film-flip-chip InGaN quantum wells light-emitting diodes with GaN micro-domes," *Energy Exp.*, vol. 20, no. S5, pp. A765–A776, Sep. 2012.
[15] P. Zhao, L. Han, M. R. McGoogan, and H. Zhao, "Analysis of TM mode light extraction efficiency enhancement for deep ultraviolet AlGaN quantum wells light-emitting diodes with III-nitride micro-domes," *Opt. Mater. Exp.*, vol. 2, no. 10, pp. 1397–1406, Oct. 2012.
[16] L. Han and H. Zhao, "Simulation analysis of GaN microdomes with broadband omnidirectional antireflection for concentrator photovoltaics," *J. Appl. Phys.*, vol. 115, no. 13, Apr. 2014, Art. ID. 133102.
[17] L. Han, T. A. Piedimonte, and H. Zhao, "Experimental exploration of the fabrication of GaN microdome arrays based on a self-assembled approach," *Opt. Mater. Exp.*, vol. 3, no. 8, pp. 1093–1100, Aug. 2013.
[18] X. H. Li *et al.*, "Light extraction efficiency and radiation patterns of III-nitride light-emitting diodes with colloidal microlens arrays with various aspect ratios," *IEEE Photon. J.*, vol. 3, no. 3, pp. 489–499, Jun. 2011.
[19] X. H. Li *et al.*, "Light extraction efficiency enhancement of III-nitride light-emitting diodes by using 2-D close-packed TiO_2 microsphere arrays," *J. Display Technol.*, vol. 9, no. 5, pp. 324–332, May 2013.
[20] C. B. Vartuli *et al.*, "Cl2/Ar and CH4/H2/Ar dry etching of III-V nitrides," *J. Appl. Phys.*, vol. 80, no. 7, pp. 3705–3709, Oct. 1996.
[21] S. Han, Z. Hao, J. Wang, and Y. Luo, "Controllable two-dimensional photonic crystal patterns fabricated by nanosphere lithography," *J. Vacuum Sci. Technol. B, Microelectron. Nanometer Struct.*, vol. 23, no. 4, pp. 1585–1588, Jun. 2005.
[22] D. Choi, H. Yu, S. G. Jang, and S. Yang, "Colloidal lithographic nanopatterning via reactive ion etching," *J. Amer. Chem. Soc.*, vol. 126, no. 22, pp. 7019–7025, Jun. 2004.